Rabi Oscillations in Landau-Quantized Graphene

Balázs Dóra,[1,*] Klaus Ziegler,[2] Peter Thalmeier,[3] and Masaaki Nakamura[1]

[1]*Max-Planck-Institut für Physik Komplexer Systeme, Nöthnitzer Strasse 38, 01187 Dresden, Germany*
[2]*Institut für Physik, Universität Augsburg, D-86135 Augsburg, Germany*
[3]*Max-Planck-Institut für Chemische Physik fester Stoffe, 01187 Dresden, Germany*

We investigate the relation between the canonical model of quantum optics, the Jaynes-Cummings Hamiltonian and Dirac fermions in quantizing magnetic field. We demonstrate that Rabi oscillations are observable in the optical response of graphene, providing us with a transparent picture about the structure of optical transitions. While the longitudinal conductivity reveals chaotic Rabi oscillations, the Hall component measures coherent ones. This opens up the possibility of investigating a microscopic model of a few quantum objects in a macroscopic experiment with tunable parameters.

PACS numbers: 73.63.−b, 72.15.−v, 81.05.Uw

Graphene, a single sheet of carbon atoms in a honeycomb lattice has attracted enormous interest recently [1]. Its quasiparticle states are pseudospinors, where the spinor structure is a consequence of the twofold sublattice structure of the honeycomb lattice (Fig. 1). They obey a two-dimensional Dirac equation, whose speed of light is replaced by the Fermi velocity (being 1/300th the speed of light). This implies a number of striking properties, including the unconventional quantum Hall effect [2], Klein tunneling [3] and *Zitterbewegung* [4–7] due to particle-hole excitations. In an applied magnetic field, perpendicular to the carbon sheet, the formation of Landau levels E_n with an unusual dependence $E_n \sim \sqrt{n}$ on the Landau level index n was predicted, and also observed experimentally [8,9].

Coupling of a (pseudo)spinor to an external quantum field is a common feature in quantum optics. In this context, one of the simplest, fully quantum mechanical model is the Jaynes-Cummings (JC) Hamiltonian[10]

$$H_{\rm JC} = V(a^+ \sigma^- + \sigma^+ a) + \Delta \sigma_z, \qquad (1)$$

which describes a single two-state atom, represented by the Pauli matrices, that is interacting with a (single-mode quantized) electromagnetic field [11]. a^+ (a) are the photon creation (annihilation) operators, and V is the coupling strength between the atom and the electromagnetic field. The interaction leads to a periodic exchange of energy between the electromagnetic field and the two-level system, known as Rabi oscillations. This effect can be interpreted as a periodic change between absorption and stimulated emission of photons. It is simply a consequence of the fact that the atom is not in an eigenstate after the absorption of n photons. A very similar situation occurs for the Landau levels of graphene. In terms of the Hamiltonian in Eq. (1), the two-level atom in the JC model (represented by σ's) corresponds to a pseudospin $1/2$ due to the two sublattices in graphene, and the photon operators a^+ and a are translated to operators in graphene that are acting on

Landau levels [12]: $a^+ = \pi^+/\sqrt{2eB}$ and $a = \pi^-/\sqrt{2eB}$, where $\pi^\pm = \pi_x \pm \pi_y$ with $\boldsymbol{\pi} = p + e\mathbf{A}$ are the (Peierls substituted) momentum operators with the vector potential $\mathbf{A}$. Formally, they act as creation and annihilation operators of a harmonic oscillator and obey a bosonic commutation relation $[\pi^-, \pi^+] = 2eB$. Moreover, the coupling constant V depends on the magnetic field strength B and the Fermi velocity in graphene $v_F = 10^6$ m/s through $V = v_F\sqrt{2eB}$. Finally, Δ represents a possible excitonic gap [13] or a substrate induced band gap [14] in epitaxial graphene. The above analogy has already been exploited in Ref. [5] when studying the classical carrier dynamics in graphene.

The pseudospinor state in the nth Landau level is not an eigenstate of the quasiparticle Hamiltonian of graphene. If we prepare an initial quasiparticle state of graphene in a certain Landau level by switching on an external magnetic field, the quasiparticles will go from the initial nonequilibrium state to other Landau levels. Depending on the damping due to (impurity) scattering, the quasiparticles oscillate between different Landau levels until they reach their equilibrium state, which is a superposition of Landau levels. Recent experiments on high-mobility samples of graphene have indicated that damping due to impurity scattering can be negligible on experimentally relevant time scales [15,16].
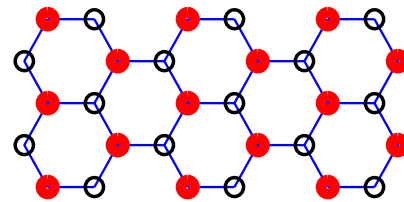

FIG. 1 (color online). A small fragment of the honeycomb lattice is shown, the filled red and empty black circles denote the two sublattices.

In this Letter we shall discuss the nonequilibrium current dynamics of high-mobility graphene. Quantum states are prepared by a short electric pulse and the subsequent current dynamics is controlled by oscillations between Landau levels.

The Hamiltonian H_{JC} can be diagonalized, and the resulting eigenvalues are obtained as $E_{n\alpha} = \alpha\sqrt{\Delta^2 + V^2(n+1)}$, where $n = 0, 1, 2 \ldots$ non-negative integer, $\alpha = \pm$. In the nonrelativistic limit ($\Delta \gg V$), the usual Landau level spectrum is obtained as $\alpha(\Delta + \omega_c(n+1))$ with the cyclotron frequency of massive (Dirac) fermions $\omega_c = v_F^2 eB/\Delta$. In addition, there is a special eigenstate, stemming from the Landau level at the Dirac point with $E^* = -\Delta$, which formally corresponds to $n = -1$ and $\alpha = -1$. Having determined the spectrum of the Hamiltonian, we turn to the investigation of the current correlations. Since $\sigma_{x(y)}$ (the pseudospin variable) is the current density in x (y) direction due to the equation of motion $j_{x(y)} = i[H, x(y)] = v_F \sigma_{x(y)}$, we can calculate the dynamical correlation function $C_{xx}(t) = \langle \sigma_x(t)\sigma_x(0)\rangle$ and $C_{xy} = \langle \sigma_x(t)\sigma_y(0)\rangle$ (symmetric and antisymmetric dipole-dipole correlator). In quantum optics, these describe the transitions between the two atomic states, and tell us about the spectrum of Rabi oscillations [17]. On the other hand, $C_{xx}(t)$ and $C_{xy}(t)$ play the role of the longitudinal and Hall current-current correlation functions in the Dirac case, and leads eventually to the optical conductivity of graphene [18,19]. Therefore, we expect the well-known Rabi oscillations of quantum optics to be observable in the response functions of Landau-quantized Dirac fermions [20].

We start with the general correlator $C(\varphi, t) = \langle \sigma_x(t)(\cos(\varphi)\sigma_x + \sin(\varphi)\sigma_y)\rangle$, evaluated using the (structureless) bosonic a operators. This defines both $C_{xx}(t) = C(0, t)$ and $C_{xy}(t) = C(\pi/2, t)$, and reads as

$$C(\varphi, t) = g_c f(E^*) \sum_{\gamma=\pm} \exp(i(E_{0\gamma} + E^*)t - i\varphi)P_{*\to 0\gamma} + \sum_{\substack{n\geq 0 \\ \alpha\gamma s=\pm}} g_c f(E_{n\alpha}) \exp(i(E_{n\alpha} + E_{n-s\gamma})t + is\varphi)P_{n\alpha\to n-s\gamma}, \quad (2)$$

where $f(E) = 1/[\exp((E - \mu)/T) + 1]$ is the Fermi function, $g_c = N_f A_c eB/2\pi$ is the degeneracy of the Landau levels including spins, A_c is the area of the unit cell, to be taken as unity in the Dirac approach, $N_f = 2$ stands for the spin degeneracy. From this, it follows immediately that a $E_{n\alpha}$ Landau level with $n > 0$ and given α possesses four possible optical transitions to the adjacent levels as $E_{n\pm 1\pm\alpha}$ (on the same side and on the other side of the Dirac cone), the $n = 0$ level three transitions to $E_{1\pm\alpha}$ and E^* and the E^* level two transitions to $E_{0\pm}$. The nonzero transition matrix elements are given by

$$P_{n\alpha\to n-s\gamma} = \frac{1}{4}\left(1 + \frac{s\Delta}{E_{n\alpha}}\right)\left(1 + \frac{s\Delta}{E_{n-s\gamma}}\right) \quad \text{for} \quad n \geq 0,$$

$$P_{*\to 0\gamma} = \frac{1}{2}\left(1 - \frac{\Delta}{E_{0\gamma}}\right), \quad (3)$$

which satisfy $\sum_{m\gamma} P_{n\alpha\to m\gamma} = 1$, and agree with the transition probabilities for Rabi oscillations of atoms induced by external electromagnetic field. These approach $1/4$ in the classical limit (of bosons) $n \to \infty$, in which case the field contains many bosons, whose quantum character can then be neglected [21]. Interestingly, the $\Delta = 0$ limit yields the classical matrix elements for any $n \geq 0$. However, the E^* level never reaches the classical limit, and is responsible for the anomalous optical properties of graphene in magnetic field [22]. The evaluation of the microwave conductivities of graphene follows readily from Eq. (2), and the response function is $\chi_{xa}(t) = -\Theta(t)2e^2v_F^2\mathrm{Im}C_{xa}(t)$, which yields to the optical ($a = x$) and microwave Hall ($a = y$) conductivity as $\sigma_{xa}(\omega) = \tilde{\chi}_{xa}(\omega)/i\omega$ upon Fourier transformation [23]. These are identical to those

[24] obtained using standard many-body techniques in the $\Gamma \to 0$ limit (where Γ is the damping [23,24]).

Equation (2), together with the relation to the JC Hamiltonian provides us with a particularly simple picture about the optical selection rules and transitions by relating them to the Rabi oscillations. Therefore, the optical conductivity by varying the frequency sweeps through all possible transitions, and measures the frequency of the Rabi oscillations, with quantum or classical character. This provides a unique opportunity to investigate a basic phenomenon of quantum electrodynamics in a condensed matter experiment. By changing the external magnetic field applied to graphene, the coupling between the atom and electromagnetic field in the JC model can be tuned continuously, facilitating the exploration of various regimes, the quantum to classical crossover.

In quantum optics, one has the freedom to prepare the initial state of both the atom and the electromagnetic field [10,11]. The atom is usually prepared in its excited state, and the field is prepared in a number state or in a coherent state [20,25]. Then one can study the time evolution of the atomic population, which exhibits Rabi oscillations, when jumping between the ground and excited state, causing collapse and revival phenomenon. However, qualitatively different behavior describes chaotic or thermal fields [26]. Quiescent periods and interfering revivals are also present, but the resulting pattern of oscillations follows an apparently random evolution. A coherent state, which is the most classical single-mode quantum state, is strongly peaked around the average boson number $\bar{n}$. Therefore, Rabi oscillations mainly involve frequencies around $E_{\bar{n}\alpha}$, and the collapse time is independent of the field strength, i.e., $\bar{n}$. As opposed to this, a thermal or chaotic field has a broad,

monotonically decreasing distribution of boson states, and
can be represented as a mixture of coherent states with a
Gaussian distribution of the mean values. As a result, the
very wide range of boson numbers gives such a broad
distribution of Rabi frequencies that almost no trace of
coherent oscillations remains after ensemble averaging,
and the resulting initial collapse time depends on the field
strength $\bar{n}$. The revival times depend on $\bar{n}$ for both initial
conditions.

For graphene, an arbitrary preparation of the initial
states is not accessible, but requires thermal, ensemble
averaging. In this respect, it is closer to the second type
of thermal initial condition for the JC model. The average
boson number in the JC model corresponds to the total
number of fermions in graphene, determined by the chemi-
cal potential and the cutoff. This can be introduced by the
energy scale $D = V\sqrt{N + 1}$, above which we neglect all
states (with $n > N$). We mention that the inclusion of a
cutoff is required to obtain correctly the f-sum rule for
graphene [27].

Using this prescription, we investigate the real-time
evolution of the longitudinal current-current correlation
function based on Eq. (2). The results are shown in
Fig. 2, including valley ($\Delta \rightarrow -\Delta$) and spin degeneracies.
Similarly to observations in quantum optics [10,26], the
initial collapse is followed by a revival of oscillation,
which are also sensitive to the presence of finite μ and
Δ. They both enlarge the quiescent period after the short
time collapse, and cause additional steplike structures in
the envelope of oscillations with a period of

$\max(\mu, \Delta)\pi/v_F^2 eB$. For longer times, collapse and revival
are observable in Fig. 3, which gradually become wider
and overlap. This revival time depends on the value of the
cutoff like $2\pi\sqrt{N + 1}/V = \pi D/v_F^2 eB$, as is apparent
from the figure, and is controllable by the magnetic field.

The Hall response ($\sigma_{xy}(\omega)$) evolves differently. In the dc
limit, by taking both valley and spin degeneracies into
account, it produces the unconventional quantum Hall
steps as a function of μ. In connection with the JC model,
these steps, occurring when μ coincides with a Landau
level energy, correspond to the bare Rabi frequencies,
which can be revealed in a static, dc experiment, but still
gaining information about the dynamics of the system. The
microwave Hall conductivity obeys to the same selection
rules and possesses the same transition matrix elements as
the longitudinal conductivity. However, the extra phase
factor in Eq. (2) is responsible for the different behavior.

The time evolution of the Hall correlator is shown in
Fig. 4, and turns out to be independent of the applied cutoff
scheme, hence being universal. It exhibits coherent Rabi
oscillations, which vanish at the Dirac point (this is equiva-
lent to the statement, that the Hall conductivity is zero
exactly at the Dirac point). Upon increasing μ, oscillations
shows up with beating property, observed in quantum
optics as well [10]. The characteristic frequency of the
envelope of the oscillations for $\mu \gg (V, \Delta)$ is $V^2/2\mu =
v_F^2 eB/\mu$, which is the cyclotron frequency of massless
Dirac fermions [2]. Even though the spectrum is linear,
the finite chemical potential provides us with an energy
scale for the cyclotron mass. Only the energy levels with
$|E_{n\alpha}| < \mu$ contribute to the Hall response at $T = 0$.
Therefore, for $\Delta > \mu$, $\mathrm{Im}C_{xy}(t) = 0$ and no oscillations
are present. This means, that only a finite, narrow range of
frequencies determine the Rabi oscillations. Thus,
although the initial field state is always a thermal one in
graphene, both coherent and chaotic Rabi oscillation can
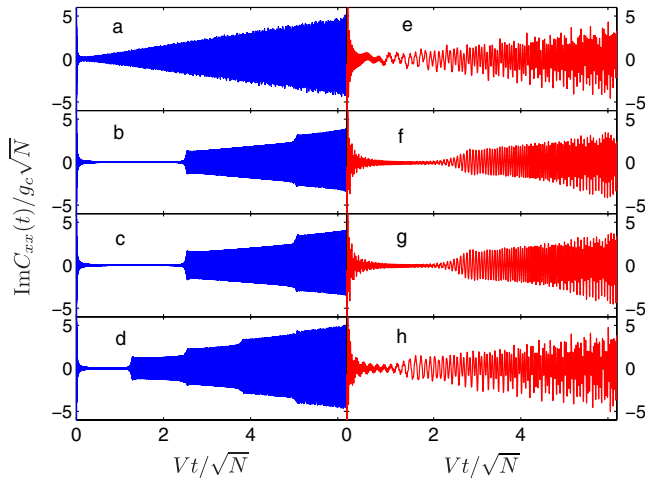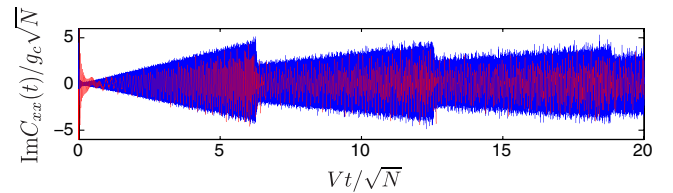be observed in different quantities, together with collapse

FIG. 2 (color online). The real-time evolution of $C_{xx}(t)$ is
shown at $T = 0$, taking both valley and spin degeneracies into
account. We introduced a cutoff D, and the number of levels is
measured as $D = V\sqrt{N}$, corresponding to different magnetic
field strengths. The left/right panels show $N = 10\,000$
(blue)/$N = 100$ (red) with $D = V\sqrt{N}$ for $(\mu, \Delta)/V\sqrt{N} = (0, 0)$
(a),(e), (0.4,0) (b),(f), (0.4,0.2) (c),(g), and (0,0.2) (d),(h). These
structures correspond to thermal field induced random oscilla-
tion in quantum optics [26].

FIG. 3 (color online). The real-time evolution of $C_{xx}(t)$ is
shown for long times for $T = 0$, $(\mu, \Delta) = (0, 0)$. We introduced
a cutoff D, and the number of levels is measured as $D = V\sqrt{N}$,
corresponding to different magnetic field strengths with $N =
10\,000$ (blue) and $N = 100$ (red). Collapse and revival shows up
with time similarly to the thermal field Jaynes-Cummings model.
The revivals gradually get wider and overlap. The presence of
thermal revivals are related to the finite average boson number in
the Jaynes-Cummings model, which translate to a finite cutoff in
the Dirac case. As opposed to Fig. 2, these revivals at long times
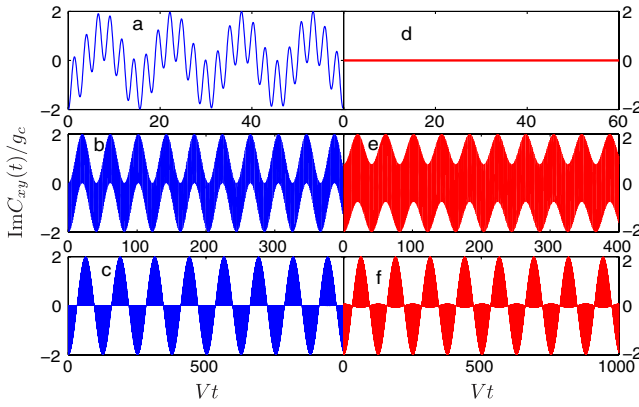are caused by the finite cutoff.

FIG. 4 (color online). The real-time evolution of $C_{xy}(t)$ is shown for $T = 0$. The explicit value of the number of levels (N) does not influence the resulting pattern. The chemical potential varied as $\mu/V = 1.2$ (a),(d), 3.2 (b),(e) and 10 (c),(f) with $\Delta = 0$ (left panel, blue) and $\Delta = 2V$ (right panel, red), and the frequency of the envelope function is $v_F^2 eB/\mu$, the cyclotron frequency of massless Dirac fermions. For $T = 0$ and $\Delta > \mu$, $\mathrm{Im} C_{xy}(t) = 0$. Note the different horizontal scales.

and revival. The correlation function $C(\varphi, t)$ measures in principle the crossover from thermal to coherent behavior with changing φ, and provides us with the unique opportunity to observe the crossover by not changing the initial field state, but by measuring a different component of the current.

Time-resolved current-voltage measurements can reveal the real-time dependence of correlation functions, similarly to the current-voltage characteristics of Josephson junctions [28]. By applying a sharp current or electric field pulse as $E = E_0 \delta(t)$, the resulting current through the sample parallel or perpendicular to E_0 after the initial pulse is directly related to the above correlation functions. More precisely, within linear response theory, it follows as $\langle j_a(t) \rangle = -2e^2 v_F^2 E_0 \int_0^t dt' \mathrm{Im} C_{xa}(t')$ with $a = x$ or y. This opens up the possibility to reconstruct the time-dependence of $\mathrm{Im} C_{xa}(t')$, or to obtain the frequency dependent longitudinal and Hall responses. Another method invokes the femto- or attosecond laser pulse technique. After shining the sample with a short laser pulse, the measurement of transmittance or reflectance in time is determined by the $C(t)$ correlation functions. The most conventional way to deduce these correlation functions is provided through optical conductivity or current fluctuation measurement. Via the fluctuation dissipation theorem, they contain the same information, and upon Fourier transforming from frequency space to get the real time dependence, one is expected to be able to observe the presence of Rabi oscillations. Similar measurements have already been carried out without magnetic field [18,19].

The above calculations can easily be extended to other correlation functions such as thermal conductivities. We also may speculate that various extensions to single layer

graphene such as bi- and multilayer structures [29] (with spin-orbit coupling) can be mapped onto different multi-mode, multiatom, and nonlinear versions of the JC model.

In conclusion, we have shown that the equivalence of the Hamiltonians of graphene in magnetic field and of the JC model influences their correlation functions as well, causing both thermal and coherent Rabi oscillation in the electric response of graphene. Finally, we speculate that Rabi oscillations and *Zitterbewegung* are two closely related phenomena named differently in different fields of physics, both arising from the coupling of positive and negative energy states.

*dora@pks.mpg.de

 [1] K. S. Novoselov *et al.*, Science **306**, 666 (2004).
 [2] K. S. Novoselov *et al.*, Nature (London) **438**, 197 (2005).
 [3] M. I. Katsnelson *et al.*, Nature Phys. **2**, 620 (2006).
 [4] J. Cserti, and Gy. Dávid, Phys. Rev. B **74**, 172305 (2006).
 [5] J. Schliemann, New J. Phys. **10**, 043024 (2008).
 [6] T. M. Rusin and W. Zawadzki, Phys. Rev. B **78**, 125419 (2008).
 [7] U. Zülicke *et al.*, New J. Phys. **9**, 355 (2007).
 [8] G. Li and E. Y. Andrei, Nature Phys. **3**, 623 (2007).
 [9] Z. Jiang *et al.*, Phys. Rev. Lett. **98**, 197403 (2007).
[10] B. W. Shore and P. L. Knight, J. Mod. Opt. **40**, 1195 (1993).
[11] S. M. Barnett and P. M. Radmore, *Methods in Theoretical Quantum Optics* (Oxford University Press, Oxford, 1997).
[12] N. M. R. Peres *et al.*, Phys. Rev. B **73**, 125411 (2006).
[13] D. V. Khveshchenko, Phys. Rev. Lett. **87**, 206401 (2001).
[14] S. Y. Zhou *et al.*, Nature Mater. **6**, 770 (2007).
[15] A. K. Geim and K. S. Novoselov, Nature Mater. **6**, 183 (2007).
[16] K. I. Bolotin *et al.*, Phys. Rev. Lett. **101**, 096802 (2008).
[17] G. S. Agarwal, J. Opt. Soc. Am. B **2**, 480 (1985).
[18] R. R. Nair *et al.*, Science **320**, 1308 (2008).
[19] Z. Q. Li *et al.*, Nature Phys. **4**, 532 (2008).
[20] M. Brune *et al.*, Phys. Rev. Lett. **76**, 1800 (1996).
[21] A. Bermudez *et al.*, Phys. Rev. Lett. **99**, 123602 (2007).
[22] T. Ando *et al.*, J. Phys. Soc. Jpn. **71**, 1318 (2002).
[23] V. P. Gusynin *et al.*, J. Phys. Condens. Matter **19**, 026222 (2007).
[24] V. P. Gusynin and S. G. Sharapov, Phys. Rev. B **73**, 245411 (2006).
[25] G. Rempe *et al.*, Phys. Rev. Lett. **58**, 353 (1987).
[26] P. L. Knight and P. M. Radmore, Phys. Lett. A **90**, 342 (1982).
[27] J. Sabio *et al.*, Phys. Rev. B **78**, 075410 (2008).
[28] J. C. Fenton *et al.*, Appl. Phys. Lett. **80**, 2535 (2002).
[29] E. McCann and V. I. Fal'ko, Phys. Rev. Lett. **96**, 086805 (2006).